Electronic Supplementary Material (ESI) for Environmental Science: Nano.

Supplementary Figures and Tables for:

Chronic exposure to complex metal oxide nanomaterials induces production of reactive oxygen species in bacteria

Deepti Sharan[1], Daniel Wolfson[2], Curtis M. Green[3,4], Paul Lemke[2], Alessandra G. Gavin[1], Robert J. Hamers[3], Z. Vivian Feng[2,5], Erin E. Carlson[1,6,7]

[1]Department of Chemistry, University of Minnesota, 225 Pleasant St. SE, Minneapolis, MN, 55454, United States
[2]Department of Chemistry, Augsburg University, 2211 Riverside Ave, Minneapolis, MN 55454, United States
[3]Department of Chemistry, University of Wisconsin-Madison, 1101 University Avenue, Madison, WI 53706, United States
[4]Process and Analytical Development, MilliporeSigma, 645 Science Drive, Madison, WI 53711, United States
[5]Council on Science and Technology, Princeton University, 1 Washington Rd, Princeton,
NJ 08544, United States
[6]Department of Medicinal Chemistry, University of Minnesota, 208 Harvard Street SE, Minneapolis, MN 55454, United States
[7]Department of Biochemistry, Molecular Biology, and Biophysics, University of Minnesota, 321 Church St SE, Minneapolis, MN 55454, United States

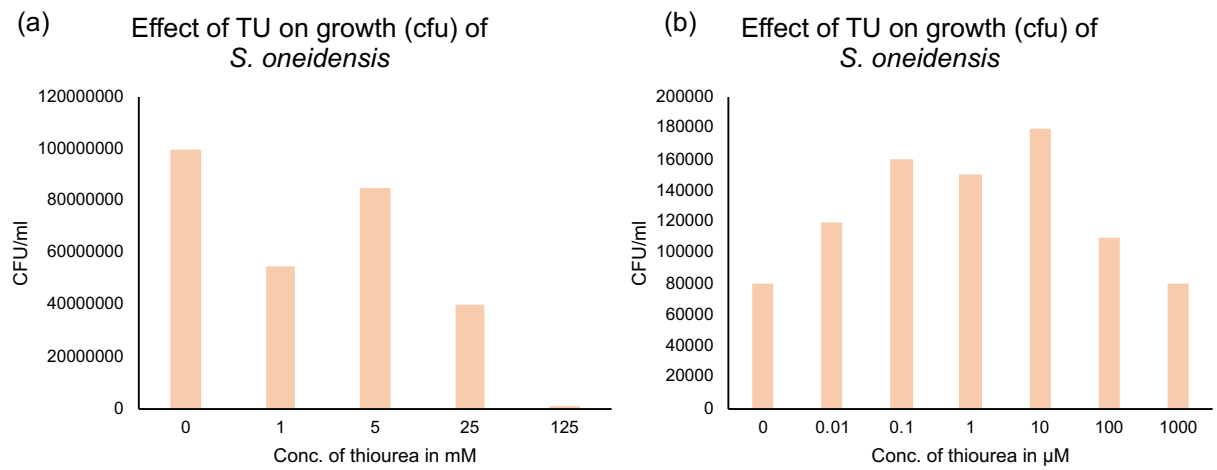

Figure S1. Determination of non-lethal concentration of ROS scavenger, thiourea (TU) in cultures of *S. oneidensis*. (a) Thiourea concentration range from 1 to 125 mM and (b) thiourea concentration in lower concentration range of 0.01 to 1000 µM.

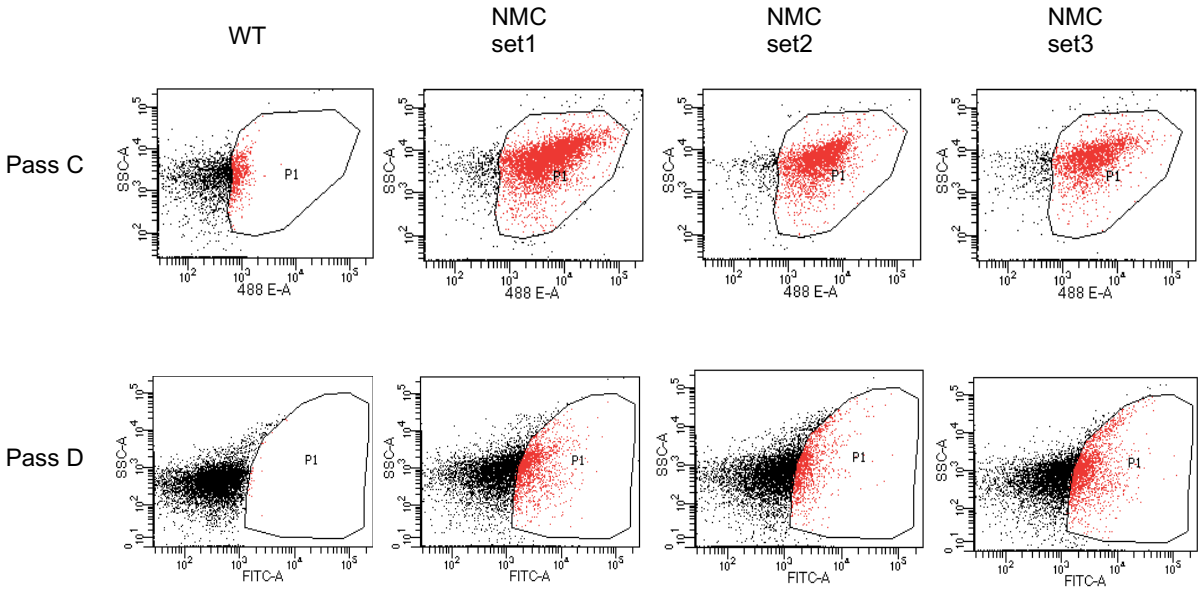

Figure S2. Flow cytometry data of DCFDA-stained cells of NMC-unexposed (WT) and NMC-exposed cultures (three biological replicates) at passage C and D.

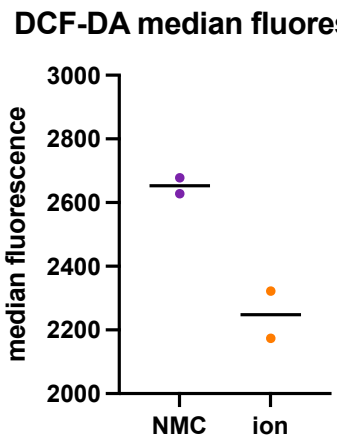

Figure S3. Flow cytometry data of DCFDA stained cells of ion-exposed and NMC-exposed cultures at passage D.

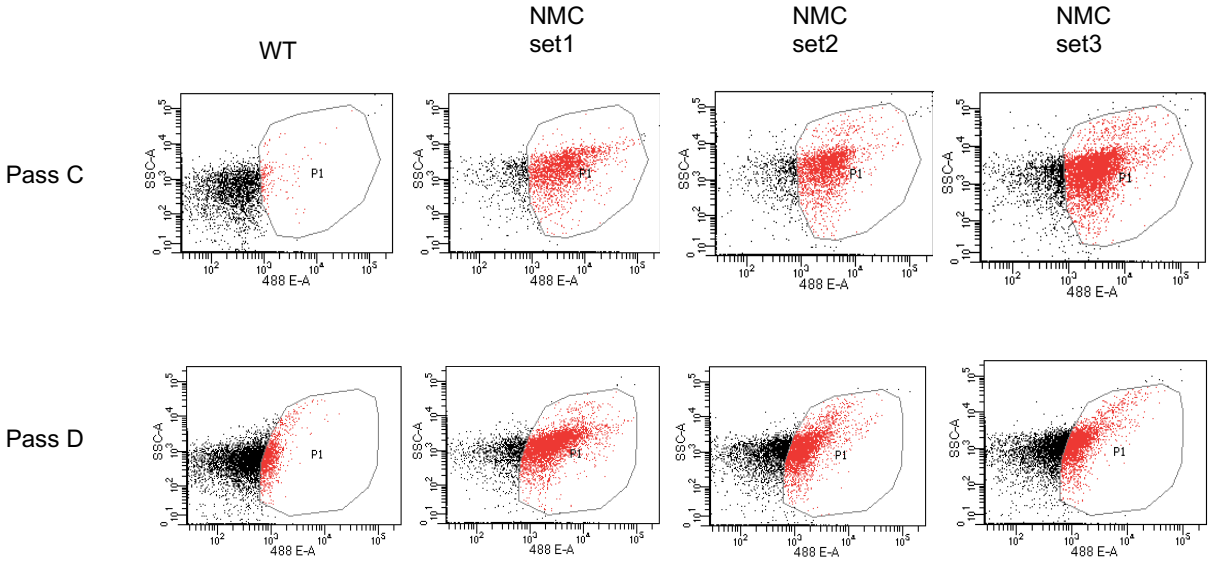

Figure S4. Flow cytometry data of HPF-stained cells of NMC-unexposed (WT) and NMC-exposed cultures (three biological replicates) at passage C and D comparing hydroxyl radical levels.

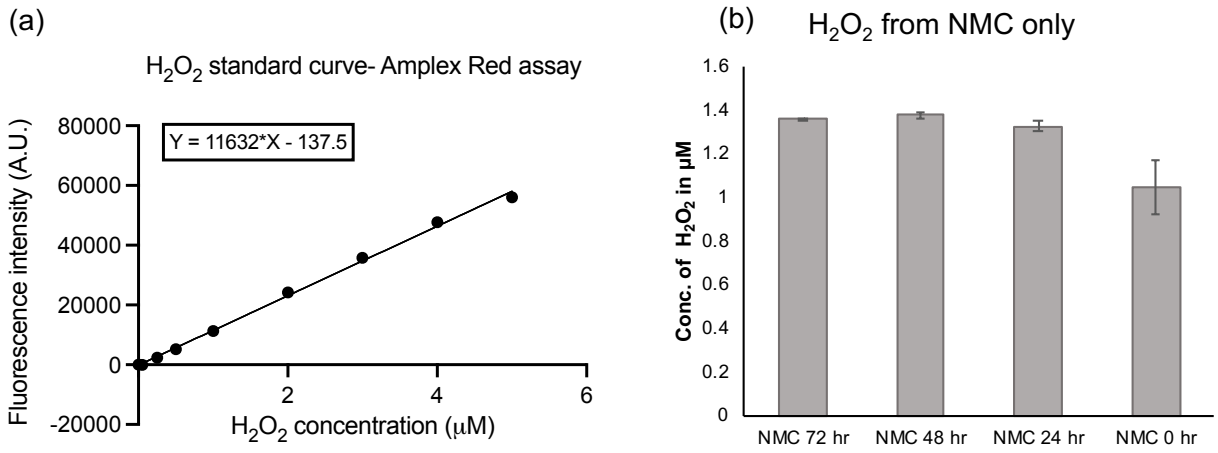

Figure S5. (a) Standard curve for H_2O_2 concentration using Amplex Red assay, as per manufacture's protocol. The H_2O_2 standard curve was plotted every time for all passages and likewise a straight-line equation was plotted for calibration. (b) Concentration of H_2O_2 as measured from NMC dispersed in minimal media over 72 hr, with measurements every 24 hr.

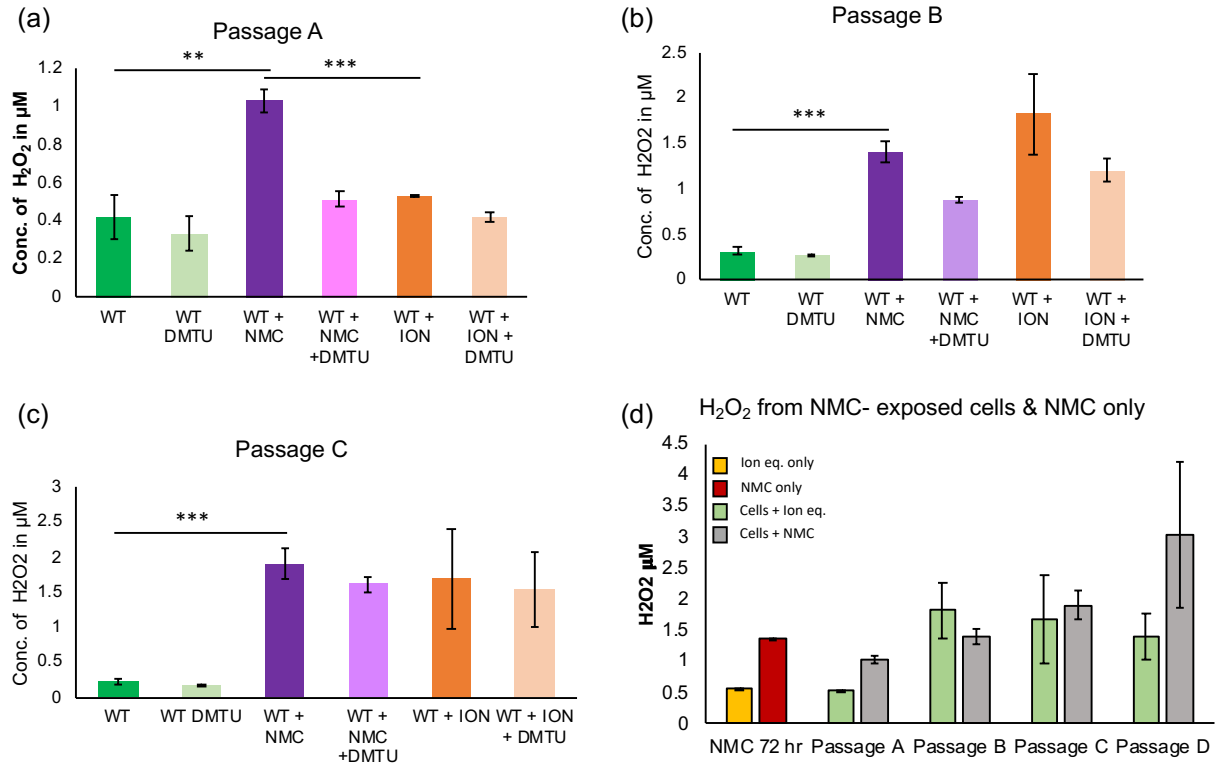

Figure S6. Determination of H_2O_2 concentration in passage A to passage C for unexposed/NMC/Ion eqv.-exposed cultures in the presence and absence of H_2O_2 scavenger dimethyl thiourea (DMTU). (a) Passage A, (b) passage B, (c) passage C and (d) comparison of H_2O_2 concentration due to NMC only, ions only with respect to when NMC/ion eqv.-exposed to the cells in cultures. Significance calculated using unpaired t-test where **, ***indicate $p \leq 0.01$, $p \leq 0.001$, respectively.

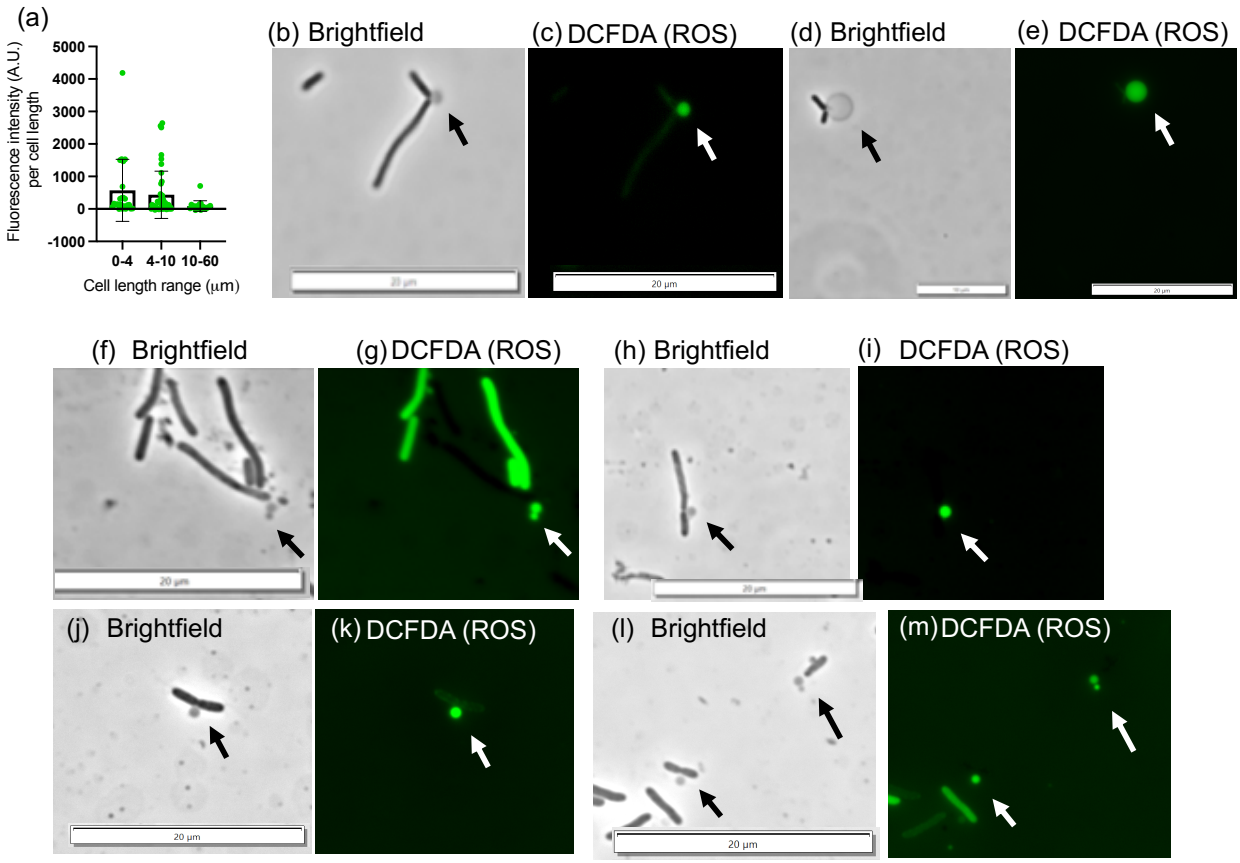

Figure S7. DCFDA-stained fluorescence imaging of NMC-exposed passage D cells. (a) Comparison of relative fluorescence intensity per unit length of cells binned according to their total cell length, (b–m) presence of vesicles in the bright field images as well as with DCFDA fluorescence.

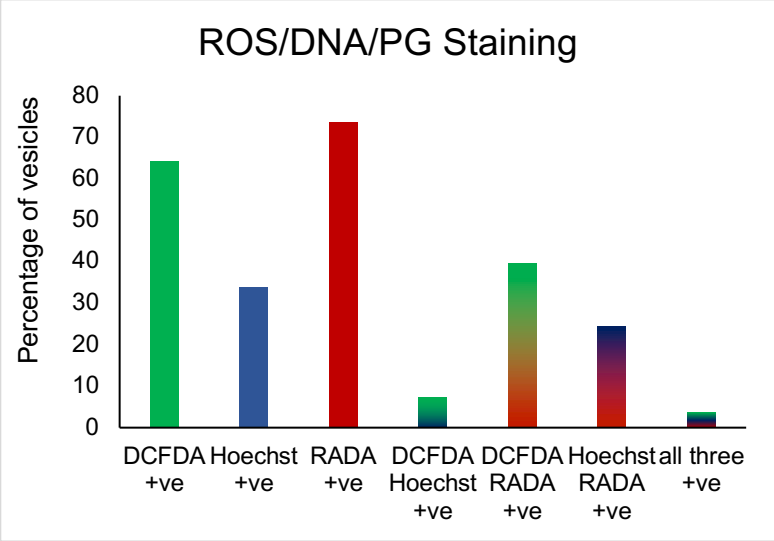

Figure S8. Graph showing percentage of vesicles from NMC exposed cultures, stained with DCFDA (for ROS), Hoechst (for DNA), RADA (for peptidoglycan) from the total vesicles (n>50) observed during the study.

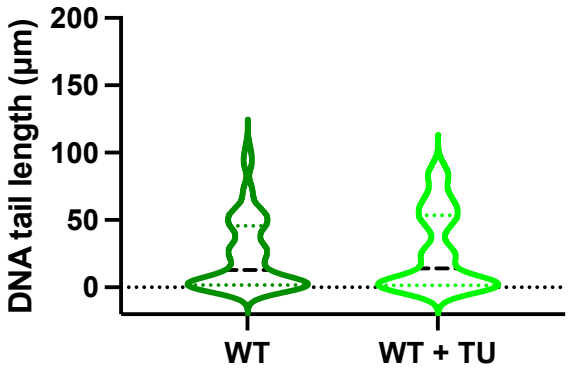

Figure S9. Comet assay bacterial tail length analysis in violin plot shows no significant changes in the extent of DNA double strand breakage in *S. oneidensis* in the presence of 0.10 mM thiourea (WT+TU) using the Kruskal-Wallis test followed by Dunn's multiple comparisons test. The dash line in the violin plot denotes the average and the dotted lines represent the quartiles (n > 90).

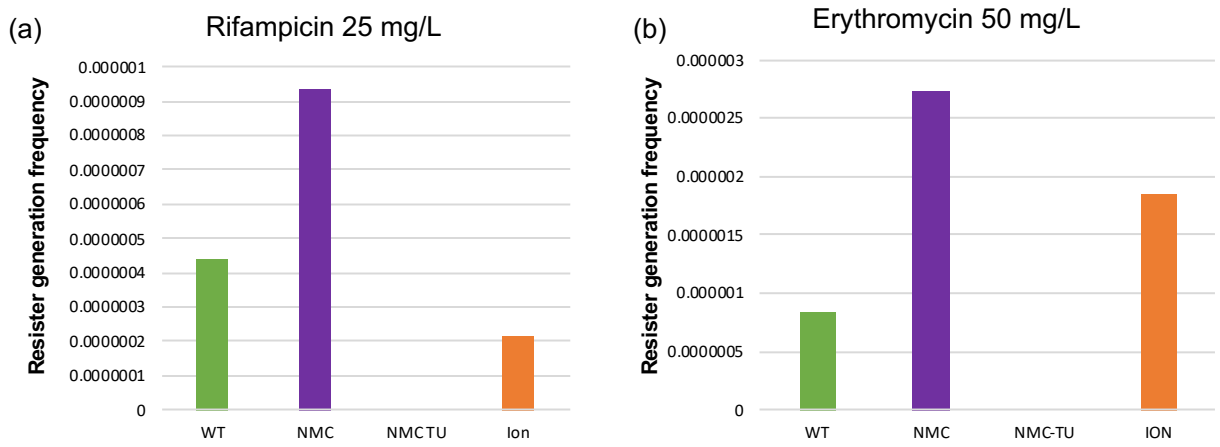

Figure S10. Resister generation frequency of cells as determined by plating on (a) 25 mg/L rifampicin and (b) 50 mg/L erythromycin.

Table S1. Point mutations in the *gyrA* gene from colonies on nalidixic acid plates.

Primer	Specificity	Sequence
Primer-QRDR-F	QRDR (gryA)	5'-gtgggacgtgcattaccaga
Primer-QRDR-R	QRDR (gryA)	5'-tgcaatacccgatgaaccgt
Primer-Rif-F	RRDR (rpoB)	5'-ttctgtgggtgagatggctg
Primer-Rif-R2	RRDR (rpoB)	5'-cacaccgtctaccactttgc
Primer-Rif-R1	RRDR (rpoB)	5'-acctactagcggcttttcagag

Table S2. Point mutations in the *gyrA* and *rpoB* genes from colonies on nalidixic acid and rifampicin plates. WT represents passaged control (without nanomaterial) and all the sequences were aligned to the sequence from the stock colonies (un-passaged).

Sample	Gene	Mutation in codon	Amino acid change	Nucleotide position	Amino acid position
WT	*gyrA*	TCG to TTG	SER to LEU	248	83
WT+NMC 1	*gyrA*	TCG to TGG	SER to TRP	248	83
WT+NMC 2	*gyrA*	TCG to TTG	SER to LEU	248	83
WT+Ion 1	*gyrA*	TCG to TTG	SER to LEU	248	83
WT+Ion 2	*gyrA*	TCG to TTG	SER to LEU	248	83
WT	*rpoB*	CGT to CTT	ARG to LEU	1589	530
WT+NMC 1	*rpoB*	CAT to TAT	HIS to TYR	1579	527
WT+NMC 2	*rpoB*	CAT to TAT	HIS to TYR	1579	527
WT+NMC 3	*rpoB*	CAA to AAA	GLN to LYS	1540	514

NMC Characterization

NMC powder was prepared for surface area analysis by heating to 120 °C under vacuum overnight. BET surface area was then measured via nitrogen adsorption isotherm (NovaTouch LX BET surface characteristic analyzer, Quantachrome, Boynton Beach, FL.). Results show NMC surface area of ~117 m^2/g.

NMC powder was prepared for XRD analysis by pressing into a B-doped zero background diffraction plate (MTI Corp, Richmond, CA). X-ray diffraction pattern was collected overnight on a Bruker D8 Advance (Bruker, Billerica, MA). The collected diffraction pattern matches the expected layered R-3m crystal structure as evidenced by comparison to $LiCoO_2$ [Citation: Kim, H.J.; Jeong, Y.U.; Lee, J.H.; Kim, J.J. Crystal structures, electrical conductivities and electrochemical properties of $LiCo_{(1-x)}Mg_xO_2$ ($0 <= x <= 0.11$). *J. Pow.* Sources 159 (2006), 233-236].

To image NMC via SEM, sample powder was suspended in isopropanol via sonication. The suspension was then dropcast on a heated B-doped Si wafer. Imaging was conducted on a Zeiss 1530 FE-SEM (Zeiss, Oberkochen, Germany) at an accelerating voltage of 5 kV. SEM images show flake-like particles with basal planes measuring ~88 (+/-) 22 nm.

To image NMC via TEM, sample powder was suspended in isopropanol via sonication. The suspension was then dropcast on a silicon nitride TEM grid (Ted Pella, Redding, CA). Particles were then imaged on a Tecnai T12 TEM (FEI) at an accelerating voltage of 120 kV. Analysis of particles viewed edge-on show the expected layered structure, with average thickness around 10 (+/-) 6 nm.

To determine material composition, 3.3 mg NMC was dissolved into 8 mL of Aqua Regia overnight. (Note: Aqua Regia is extremely corrosive and releases toxic gases, use extreme caution). An aliquot of the resulting solution was then diluted. The concentrations of each metal were then measured using ICP-OES (Agilent 5110, Agilent, Santa Clara, CA). Measurements were converted from parts per million to molarity. Composition was then determined by dividing the metal concentration by the sum of the nickel, manganese, and cobalt concentrations. This led to a composition of $Li_{0.65}Ni_{0.35}Mn_{0.32}Co_{0.33}O_2$.

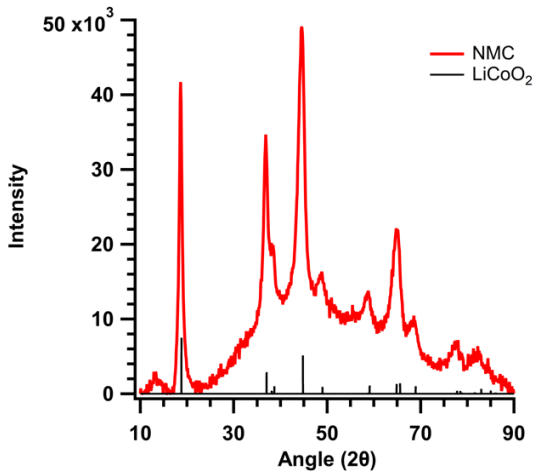

Figure S11. NMC XRD pattern. Collected diffraction pattern matches expected R-3m crystal structure.

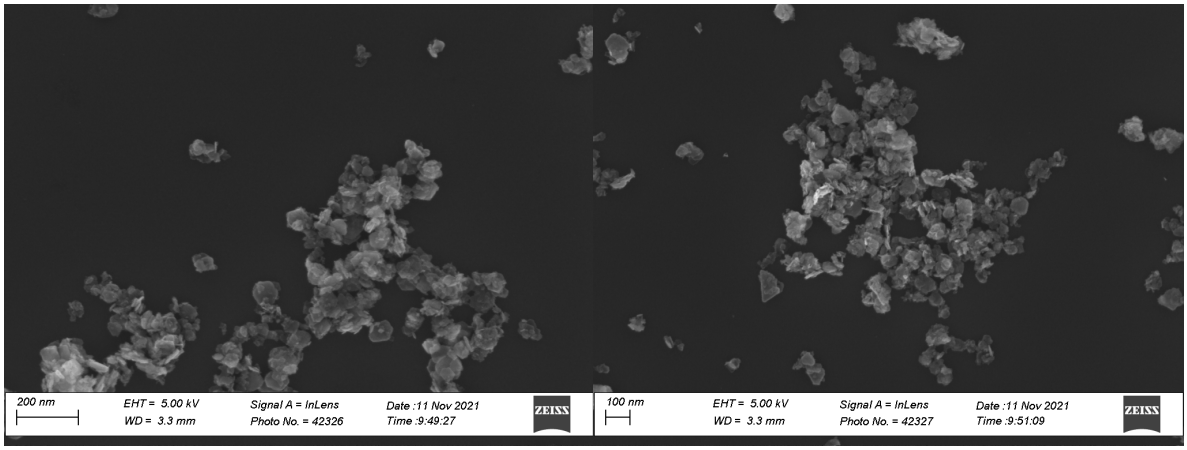

Figure S12. Imaging of NMC by SEM.

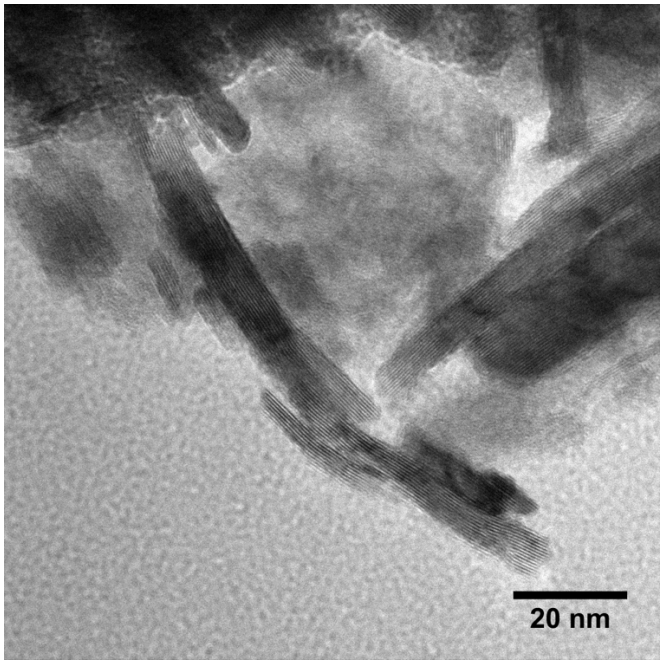

Figure S13. Imaging of NMC by TEM.